

Proficient Remote Sensing Method using GEE-SAR Data Analysis for Early Flood Disaster Mapping in Sri Lankan Major River Basins

Kumarayapa Y A A, Bandara A S

Department of Electronics, Wayamba University of Sri Lanka, Kulitapitiya, Sri Lanka

Abstract: Although, there are high population densities living around some of the major river basins due to the fertility of the areas, even in the case of minor floods, these settlements are constantly at risk due to flow of this excess water to the Dry Residential Areas. When such over-flooding occurs in the river basins, it is important to have real-time remote mapping, causality determination, and analyzing method to prevent disasters and to deploy emergency response teams to rescue human lives. Nevertheless, the use of aerial images for geographical mapping of such critical areas is difficult and unclear due to the cloudy atmosphere that exists with heavy rainfall and other environmental disturbances. To circumvent such obstacles, we propose a novel method that employs Sentinel 1 SAR data, as well as a speckle filter, to further refine the critical flood events over a free-defined period. Compared to the existing optical sensing methods (MODIS, Landsat etc.), the proposed method gives more accuracy in data analysis and prediction. In land cover classification test, it achieves 94.41% accuracy. The method combined with user-friendly GEE-SAR based platform, foremost over normal aerial photograph analysis as it avoids any environmental disturbances. Thus, the general public here without computer literacy can be informed timely about the threats via phones, etc. Hence, this research study with our novel risk identification method and formulated applet will protect those lives near the rivers. The proposed methodology based approach can be used for flood daunted river basins exist anywhere in the world

Keywords: Flood mapping, Remote Sensing, Synthetic Aperture Radar (SAR), speckle filter, image feature extraction

I. INTRODUCTION

Floods are natural disaster that occurs regularly in many parts of the world. Generally, a flood occurs when the water level of a river exceeds its maximum water level, and this excess water flowing into dry areas is called a flood [1]. Floods are the most unfavorable structure of natural risks in each local and global context. This is actually in phrases of every loss of existence and property damage. In Sri Lanka too, floods are more common than any other natural hazard [2]. When considering the early major flood hazard in Sri Lanka, 14-16 May 2021 Heavy rains and winds resulted in flooding in several districts with Colombo, Gampaha, and Galle being the worst affected with a high range of damages and displacements. A whole of 43,493 humans was affected in all districts [3]. In the month of May 2021, this flash flood occurred due to Cyclone Yaas which originated in the Bay of Bengal. According to Sri

Lanka's Disaster Management Centre (DMC) report dated 6 Jun 2021, the above-mentioned floods killed at least 4 human beings, and also about 42000 human beings had been affected. Moreover, around 200 homes had been completely or in partly broken through the floods in May 2021.

While precipitation forecasting and a flood early warning device continue to be central to a pre-disaster hazard administration strategy, post-disaster speedy response in phrases of flood detection, characterization, and injury evaluation stays central to the administration of excessive occasions such as floods [4]. At present, there are different types of flood hazard mapping techniques used for watershed management, hazard assessment on a local level, emergency planning and management, planning of technical measures, taking flood insurance, and underwriting of flood risk [5].

Also, the hydrologists used a different technique to map flood in effected areas to reduce human and property losses. Earlier the flood submerged area on the ground images were captured using observatory aircrafts. Then after analyzing the effect on the Region of Interest (ROI) of the acquired areal images, reaching the area by hazard rescue teams is a commonly used procedure in other countries [6] and in Sri Lanka. However, with the difficulties in reaching the flooded area, due to blockage by fallen electric and communication networks poles, it is difficult to monitor the flood-affected area for emergency response, thus this procedure is risky for the effected population as well it time consuming.

With the advancement of computer resources and the field of remote sensing satellite image, analysis-based flood mapping could be used effectively to inundate flood mapping in past. MODIS data and Landsat 8 data based on different flood inundation technologies existed. Since most flood events are caused by heavy rainfall, optical imagery (e.g., from MODIS and Landsat) has limited applications due to rain cloud coverage, hence the image results are not that accurate. [7]. Therefor compared to available literature, the proposed flood mapping with its formulated applet based proficient remote sensing river basin risk identification method will be a feasible solution for the above-mentioned problems.

Hence, in this research work a real time flood mapping and monitoring online web-based application developed on Google Earth Engine (GEE) platform by using the SAR data sets

(Fig.1). Also, in this research work, SAR data is used to identify the inundated pixels before and during the flood to determine the extent and damage caused by the flood. Moreover, the new web application is presented here that allows the rural user to map the flood quickly, the general public without much technical knowledge to be informed via phone alerts and by other medias such as radio broadcast etc.

II. METHODOLOGY

A. Focused study River Basin areas and related Rainfall data level

Sri Lanka lies between 6° and 10°N latitude and between 80° and 82°E longitude in the Indian Ocean, with a land region of almost 65,610 km² and a populace of 20 million. With a tropical monsoon climate, there are two principal durations of rainfall: the northeast monsoon brings rainfall to the Northern and Eastern areas in December and January; and the southwest monsoon brings rainfall to the western, southern and central areas from May to July. The incidence of floods is primarily due to heavy rainfall because of the improvement of low stress in the Bay of Bengal. Western, Southern and Sabaragamuwa provinces are the most affected via the popular floods all through the southwest monsoon. The Eastern, Northern and North central provinces are affected for the duration of the northeast monsoon. Most of the rivers originate from Sri Lanka’s mountainous central location and go with the flow outwards in all instructions down to the sea. According to the data of disaster management system of Sri Lanka, Kelani, Mahaweli, Gal Oya, Nilwala and Deduru oya river basins are the most flood prone areas which depicts in the following Figure 1 (: The most flood prone river basins study areas).

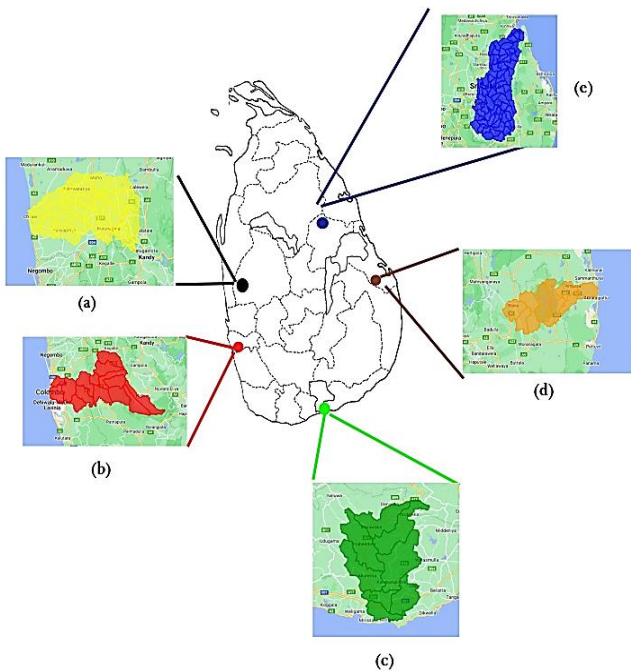


Fig. 1 The most flood prone river basins study areas (a) Gal Oya river basin. (b) Kelani river basin (c). Nilwala river basin, (d). Deduru Oya river basin, (e). Mahaweli river basin

B. GEE Rainfall data extraction

GEE is a cloud-platform for earth data analysis. It stores petabytes of archived satellite imagery and raster data and enable user to perform analysis on these data on the server side through APIs, and using huge computing power some of the potential applications are environmental monitoring, earth sciences, deforestation, etc. [8]. Nevertheless, it does not give local river basin data and remote sensing images without formulating new coding-based application platform. Thus, using following formulated coding on GEE code editor, the required data was extracted. Moreover, the following two graphs were plotted in order to illustrate the variation of monthly rainfall dataset we focused for our research the rain period in 2021; (a) for Precipitation and (b) for generate linear fit model of the graph (a).

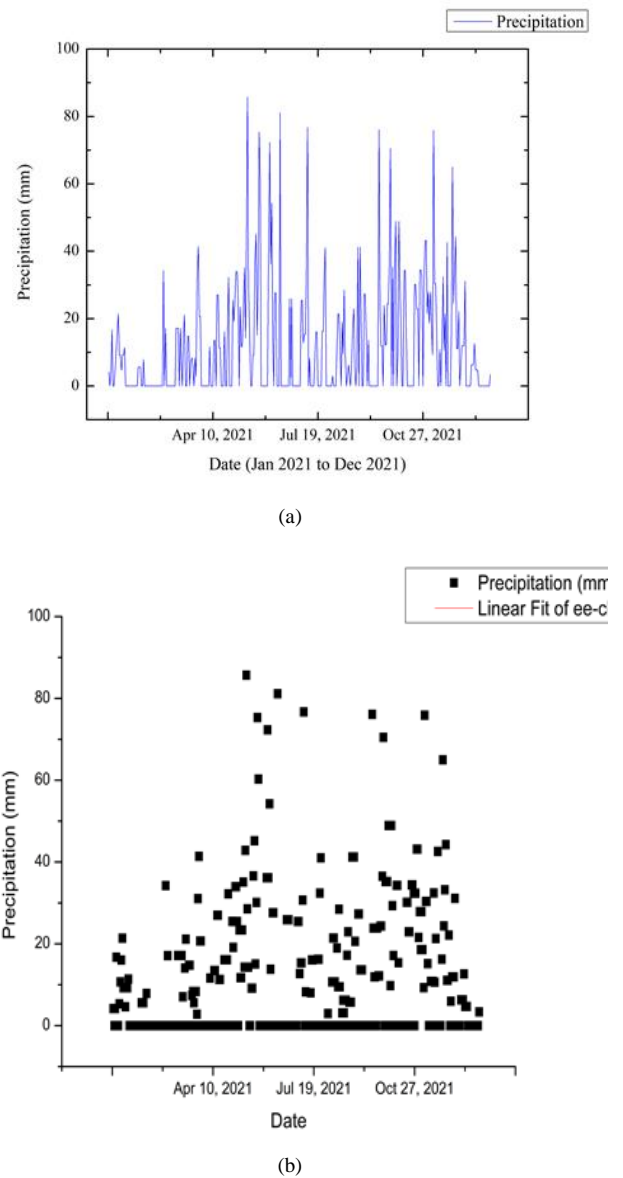


Fig. 2 Variation of monthly rainfall data set in 2021 (a) Precipitation (b) Generated Liner fit modal graph for (a)

C. The GEE data Classification

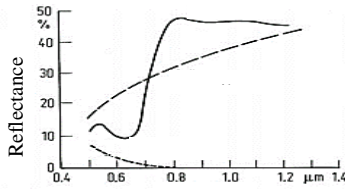


Fig. 3 Spectral reflectance of Vegetation, Soil and Water in different Wavelength

Identification of features in remote sensing imagery by photointerpretation is effective for global assessment of geometric characteristics and general appraisal of ground cover types. It is however, impracticable to apply at the pixel level unless only a handful of pixels is of interest [9].

Also, spectral reflectance of Vegetation, Soil and Water in different wavelength can be cross referenced in the following illustrated graph.

D. Image Histogram Analysis

In SAR remote sensing image, each pixel with a given brightness versus wavelength value can be constructed. This is referred to as the histogram visualization of the image. An image has a unique histogram but the reverse is not true in general since a histogram contains only radiometric and no spatial information. One important point of this analysis is that the histogram can be viewed as a discrete probability distribution as the relative height of a particular bar can be normalized by the total number of pixels in the image segment, which indicate the chance of finding a pixel with that particular brightness value somewhere in the image [9].

F. Image Smoothing with Filtering

Images can contain random noise superimposed on the pixel brightness values owing to noise generated in the sensors that acquire the image data, systematic quantization noise in the signal digitizing electronics and noise added to the video signal during transmission. This will show as a speckled ‘salt and pepper’ pattern on the image in regions of homogeneity; it can be removed by the process of low pass filtering or smoothing. Typically, this can be done at the expense of some high frequency information in the image. Nevertheless, we choose the speckle filter in this research work, in order to preserve original information in the RS images by eliminating such noises.

1) Speckle filtering-based noise reduction done at data pre-processing:

Speckle noise is a common phenomenon in all coherent imaging systems like laser, acoustic and SAR imagery. The source of this noise is attributed to random interference between the coherent returns issued from the numerous scatters present on a surface, on the scale of a wavelength of the incident radar wave. Speckle noise is often an undesirable

effect, especially for Automatic Target Recognition (ATR) systems. Thus, speckle filtering turns out to be a critical pre-processing step for detection water body areas and for classification and optimization of SAR data in this research. Moreover, SAR speckle reduction techniques fall into two categories: non-coherent (or multi-look integration) and adaptive image restoration techniques (post-image formation methods). In our research we used the non-coherent noise reduction method.

2) Speckle Filter based Statistical analysis

Fully developed speckle has the characteristics of a random multiplicative noise. under the assumption that the real and imaginary parts of the speckle have zero-mean Gaussian density, the noise intensity follows a Gamma distribution (which reduces to an exponential distribution for single-look images). The usual way to estimate the speckle noise level in a SAR image is often termed the Equivalent Number of Looks (ENL), using pixel intensity values over a uniform image area. Unfortunately, the ENL carries no information on the resolution degradation and because of that, we will use it jointly with the Signal-to-Mean-Square Error Ratio (S/MSE) which is given by,

$$10 \log_{10} \frac{\sum_{pixels} (I_1)^2}{\sum_{pixels} (I_2 - I_1)^2} \dots \dots \dots (1)$$

, where I_1 and I_2 are the un-noisy and noisy images, respectively) which corresponds to the standard SNR in the case of additive noise.

3) Rayleigh Speckle Models

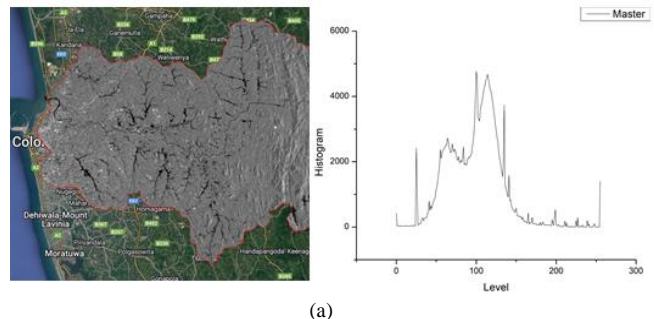
Consider a large number of scatters in a resolution cell. The received signal is a vector sum of waves reflected from the scatters. Let x and y denote its real and imaginary components. The intensity I , defined as $I = x^2 + y^2$, is exponentially distributed,

$$P_1(I) = \frac{1}{\sigma^2} \exp\left(-\frac{I}{\sigma^2}\right) \dots \dots \dots (2)$$

With mean $M1(I) = \sigma^2$, and variance $var1(I) = \sigma^4$. The amplitude, A which is the square root of I , has a Rayleigh distribution (8-Richards & Jia, n.d.),

$$P_1(A) = \frac{2A}{\sigma^2} \exp\left(-\frac{A^2}{\sigma^2}\right) \dots \dots \dots (3)$$

The following image signal analysis illustrate the effect of above filtering process



(a)

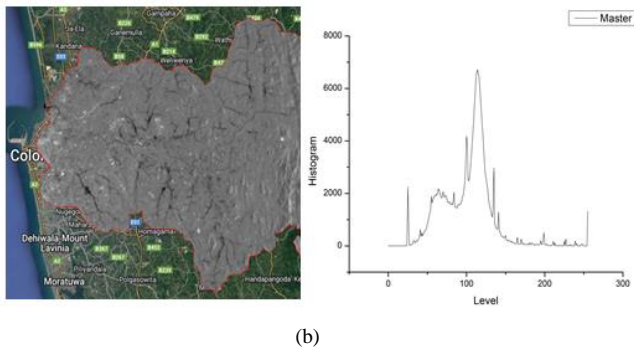


Fig. 4: Over the Kalani river basin (a) Flooded water area and its histogram before applying speckle filter. (b) Flooded water area and its histogram after applying speckle filter

E. novel methodology approach for flood and disaster rapid analysis

The proposed novel approach methodology for flood and disaster rapid analysis for faster response to save lives and their belongings consist of the following steps. The overall methodology with its sub functional processing steps was illustrated in Figure 07) dataflow diagram at the section E(6).

1) *Loading and filtering the GEE data set* : with the log scaling data of the detected, Sentinel-1 SAR: C-band Synthetic Aperture Radar for Ground Range Detection (GRD)

The Sentinel-1 mission consists of 2 satellites. Sentinel – 1 A and Sentinel – 1B and these satellites operates on c-band (5.405GHz) Synthetic aperture radar (SAR) sensors. Also, it implies spatial resolution of 10m. Sentinel – 1 can be configured to receive specific polarizations simultaneously. It can transmit a signal in either horizontal (H) or Vertical (V) polarization, and then receive in both H and V polarization bands [10].

- HH: horizontally transmitted, horizontally received.
- VV: vertically transmitted, vertically received.
- VH: vertically transmitted, horizontally received.
- HV: horizontally transmitted vertically received.

2) *WWF HydroSHEDS Basins Level 12 Dataset*

HydroSHEDS is a mapping product that provides hydrographic information for regional and global-scale applications in a consistent format. It offers a suite of geo-referenced datasets (vector and raster) at various scales, including river networks, watershed boundaries, drainage directions, and flow accumulations. HydroSHEDS is based on elevation data obtained in 2000 by NASA's Shuttle Radar Topography Mission (SRTM). This dataset provides polygons of nested, hierarchical watersheds, based on 15 arc-seconds (approx. 500 m at the equator) resolution raster data. The watersheds range from level 1 (coarse) to level 12 (detailed), using Pfaster codes.

The following JavaScript code segments were formulated for loading Sentinel 1 data set and filtering the data from geometry specifications.

```
function imgCollection(geometry){
var collection= ee.ImageCollection("COPERNICUS/S1_GRD")
.filter(ee.Filter.eq('instrumentMode','IW'))
.filter(ee.Filter.listContains('transmitterReceiverPolarisation', 'VH'))
.filter(ee.Filter.eq('orbitProperties_pass', 'DESCENDING'))
.filter(ee.Filter.eq('resolution_meters',10))
.filter(ee.Filter.bounds(geometry))
.select("VH");
return collection;
}
```

Fig.5 The JavaScript code segments utilized in 1).

3) *Visualization of RGB composite*

A SAR image can be visualized as a multi-band RGB image. In RGB composite the VV band used in red channel, the VH band used in the green channel and the VV/VH band used in the blue channel.

The bands have different min and max values, so we can visualize the images in various format with respect the min and max values. As given in above Fig 5 , for this task also the code was formulated for extracting the RGB composite of the specified geometry.

4) *Application of Speckle Filter*

The related JavaScript functions were executed for applying speckle filter to remove noise in the datasets (and can be provided the 15 lines long as requested).

5) *Application of the Mask*

The initial flooded map shows all the areas that the water is recorded. But this contains both noise and permanent water. By applying the mask, we can mask out the Region of Interest (ROI) pixels which only contain flood water.

The following JavaScript code segments were formulated for executing the flooded area after applying the mask.

```
// Remove isolated pixels
// connectedPixelCount is Zoom dependent, so visual result will vary
var connectedPixelThreshold = 8;
var connections = flooded.connectedPixelCount(25)
var disconnectedAreas = connections.lt(connectedPixelThreshold)
var disconnectedAreasMask = disconnectedAreas.not()
var flooded = flooded.updateMask(disconnectedAreasMask)
var layer9 = ui.Map.Layer(flooded, {min:0, max:1, palette: ['orange']}, 'Flood Area',
false)
c.map.layers().set(9,layer9)
```

Fig.6 The JavaScript code segments utilized in 7).

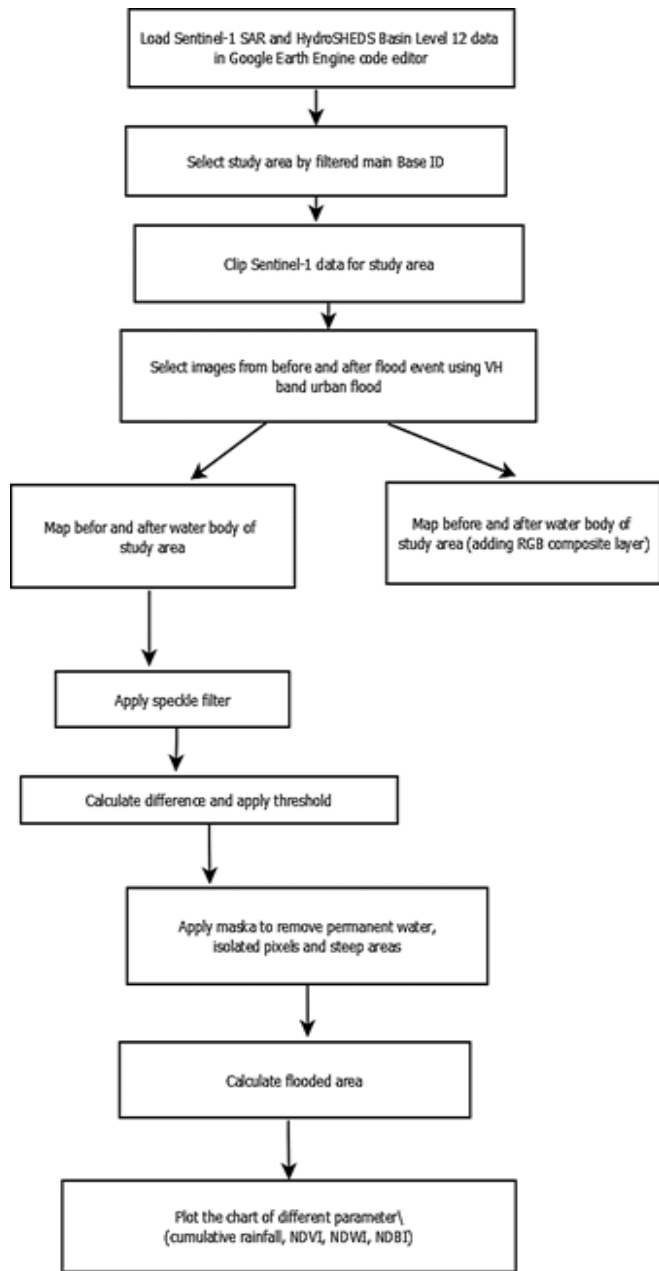


Fig. 7 The data flow diagram of the overall stepwise approach of the proposed methodology (section 6 below)

6) *The data flow diagram for clarifying the overall procedure associated with the navel method*

The above (page5) data flow diagram illustarte the overall stepwise approach of the proposed methodology for identifying flooded areas with its sivereness to immidially rescue the people and their belonging soon as possible .

III. RESULTS AND DISSCUSSION

A. *Floded Area Evaluateion*

The following table shows the calculated flooded area and total area of major river basins on time period from 10-04-2021 to 04-05-2021.

Table 1: Calculated Flooded Area Percentage

River basin	Total Area (Ha)	Flooded Area (Ha)	Flooded Area (%)
Kelani gange	232532	9953	4.28
Nilwala ganga	104142	6358	6.10
Deduru oya	347293	15839	4.56
Mahaweli ganga	1016117	45629	4.49
Gal oya	172267	7950	4.61

The following graph further illustrate the flooded area evaluated during the major flooding focused under the research study.

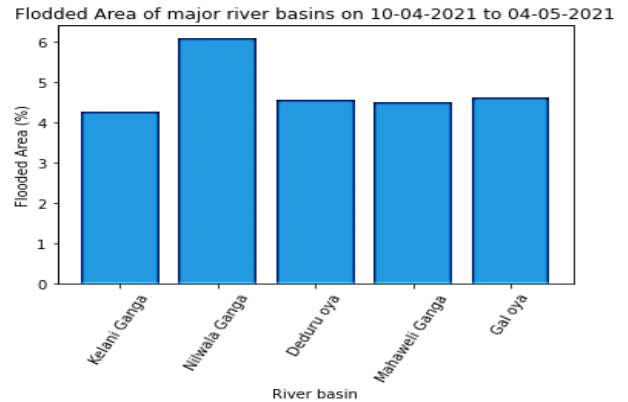


Fig. 8 The bar chart of flooded area in different river basins during 2021.

B. *The Arial Flooded Area Mapping with the navel approach*

In order to evaluate the efficiency and reliability of the proposed remote sensing method, initially the Kelani River basin was focused. The Figures 9(a) before the hazardous flood period during 2021, 9(b) after the flood and 9(c) after applying the proposed method with the filter and the mask discussed above under section F. The user interface given in Fig.9 designed for visualizing and testing the results of the navel method based on HVS method and with respect to image classification test.

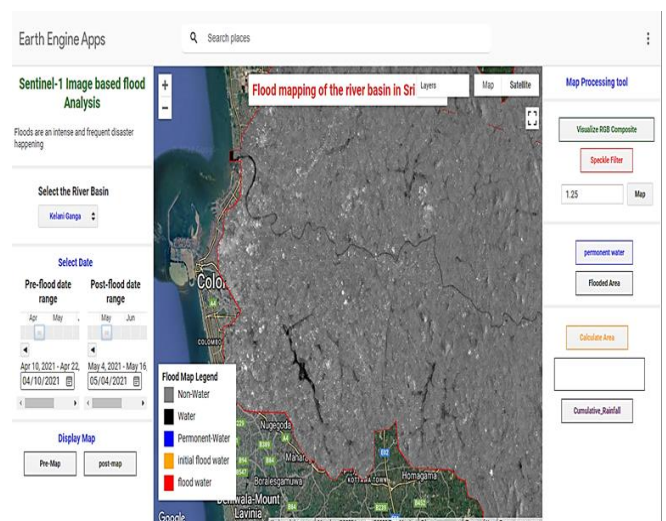


Fig. 9 (a) The areal map for Kelani River basin before the flood within the time period of 04/10/2021- 04/05/2021

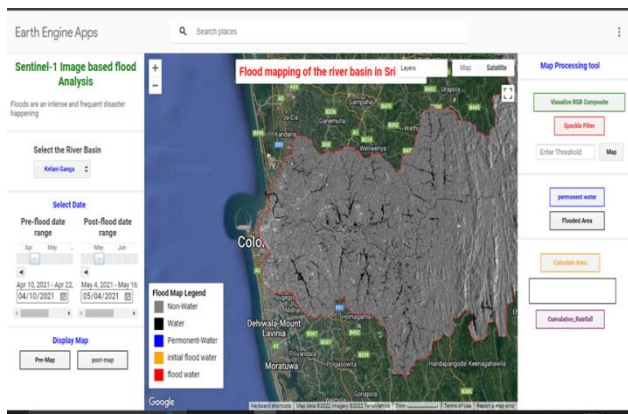


Fig.9 (b) The areal map for Kelani River basin after the flood within the time period of 04/10/2021- 04/05/2021

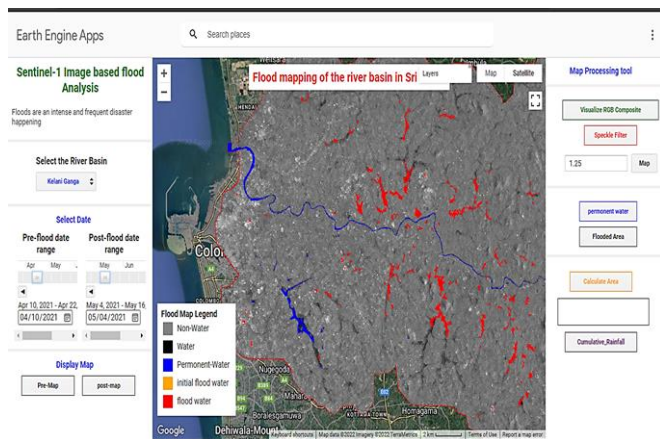


Fig. 9 (C) The map of extracted hazardous flooded area in Kelani River basin after applying filter and mask with the time period of 04/10/2021- 04/05/2021

Moreover, according to our novel method, the above 9(C) processed image can be used to extract flood effected area with Region Of Interest (ROI) ground truth [6] using more HVS identification ability with red color.

C. Image data Classification Test

The following java script code segments were formulated to calculate the accuracy in image classification and the results of confusion matrix also generated, which also nearly clarified by HVS test results, in the context of all five river basins.

```

49
50 // Classify the image.
51 var classified = composite.classify(classifier);
52
53 Map.addLayer(classified, {min: 0, max: 3, palette: ['gray', 'brown', 'blue', 'green']}, 'classified');
54
55 //*****
56 // Accuracy Assessment
57 //*****
58
59 // Use classification map to assess accuracy using the validation fraction
60 // of the overall training set created above.
61 var test = classified.sampleRegions({
62   collection: validationGcp,
63   properties: ['landcover'],
64   tileScale: 16,
65   scale: 10,
66 });
67
68 var testConfusionMatrix = test.errorMatrix('landcover', 'classification')
69 // Printing of confusion matrix may time out. Alternatively, you can export it as

```

Fig. 10 The coding used for in image classification

Use `print(...)` to write to this console.

Confusion Matrix

```

▼ [[41,4,0,0],[3,43,0,0],[0,0,48,3],[0,0,0,37]]
  ▶ 0: [41,4,0,0]
  ▶ 1: [3,43,0,0]
  ▶ 2: [0,0,48,3]
  ▶ 3: [0,0,0,37]

```

Test Accuracy

0.9441340782122905

Fig. 11 The generated results for image classification test

IV. DISCUSSION

In this research work the novel SAR data analysis and visualization method is introduced based on GEE platform. The proposed method was tested considering the data for the year 2001 major flooding occurring period due to Cyclone Yaas which originated in the Bay of Bengal. The Figures: 9 to 11 were used depict the accuracy and validity of the proposed method using machine processed identification results. More over the machine processed result further clarified using Human Visual System (HVS) based effected area identification test; 89% using ten (10) academic person's vision.

In the second stage of further implementation, this method will be combined with the proposed soil condition assessing sensor-based electronic automation system together with IOT network which will also be helpful to analyze and predict the landslide prone earth areas of the major river basins.

V. CONCLUSION

This research work formulated novel approximately real time basis method for the critical river basin flood area mapping and problem identification using rapid stepwise approach by processing remotely sensed SAR data with conjunction of GEE. Compared to the existing optical sensing methods (MODIS, Landsat etc. [11]), the proposed method gives more accuracy in data analysis and prediction. The accuracy and reliability of the novel method verified using machine based accuracy test with 94.41% of land cover image data classification test accuracy as well with HVS based testing (with 89%).

Hence, the general public (even without much computer literacy) living in those dangerous rural areas attached to the river basins can be informed either by SMS, radio or other means about the state of flood and places that are safer for their lives and to safeguard the belonging valuable things. The other major advantage of this method (with its designed user interface Applet for Google Earth Engine) is that the rapid extraction of flood data with respect to the rainfall data variation.

ACKNOWLEDGEMENT

The authors appreciatively acknowledge the flood and related information given by Disaster Management Center and weather data given by Department of Meteorology, Sri Lanka

REFERENCES

- [1] Sivakumar S.S. Flood Mitigation Strategies Adopted in Sri Lanka A Review; Journal of Scientific & Engineering Research, vol.6, Issue 2, February 2015, p 607
- [2] UNDP BOOK CHAP 04_ Flood.pdf, Available at http://www.dmc.gov.lk/images/hazard/hazard/Report/UNDP%20BOOK%20CHAP%2004_%20Flood.pdf, (accessed on 20 July 2022)
- [3] Alahacoon, N., Matheswaran, K., Pani, P., & Amarnath, G., A decadal historical satellite data & rainfall trend analysis (2001-2016) for flood hazard mapping in Sri Lanka. Remote Sensing, 2018 vol.10(3), DOI:<https://doi.org/10.3390/rs10030448>, 16–23.
- [4] Kokularamanan, S., Development of A Flood Forecasting and Data Dissemination System for Kalu River Basin in Sri Lanka, vol. 1, 1–6. Available at <https://www.pwri.go.jp/icharm/training/master/img/2016/synopses/mee15633.pdf>, (Accessed on 2nd September 2022)
- [5] Luke A, Sanders BF et al, Going beyond the flood insurance rate map: Insights from flood hazard map co-production, Natural Hazards and Earth System Sciences, 2018, doi.org/10.5194/nhess-18-1097-2018, 1097-1120
- [6] Kumarayapa, A., Zhang, Y. More efficient ground truth ROI image coding technique: implementation and wavelet-based application analysis. J. Zhejiang Univ. - Sci. A, 2007; DOI: https://doi.org/10.1631/jzus.2007_A0835, vol.8, 835–840
- [7] Lehner, B., Grill, G., Global river hydrography and network routing: Baseline data and new approaches to study the world's large river systems. Hydrological Processes 2013; DOI:<https://doi.org/10.1002/hyp.9740>, 27(15), 2171–2186
- [8] Gandhi, Ujaval, Google Earth Engine for Water Resources Management Course; Spatial Thoughts, 2021. Available at <https://courses.spatialthoughts.com/gee-water-resources-management.html>, (Accessed on 12 May 2022)
- [9] Richards, J. A., & Jia, X., Remote Sensing Digital Image Analysis. 4th edition, Springer Science and Business Media, Inc., New York, USA
- [10] Sentinel 1 SAR; Google Earth Engine, 2021, Available at <https://developers.google.com/earth-engine/guides/sentinel1>, (Accessed on 26 June 2022)
- [11] Song, X.-P., Huang, W., Hansen, M. C., Potapov, P., An evaluation of Landsat, Sentinel-2, Sentinel-1 and MODIS
- [12] data for crop type mapping. Science of Remote Sensing, January 2021, vol.3, DOI: <https://doi.org/10.1016/j.srs.2021.100018>